SAND-76-0527
Unlimited Release

# A TWO-DIMENSIONAL VISCOELASTIC MODEL FOR USE IN FINITE DIFFERENCE CALCULATIONS

J. W. Swegle

Prepared by Sandia Laboratories, Albuquerque, New Mexico 87115 and Livermore, California 94550 for the United States Energy Research and Development Administration under Contract AT (29-1)-789

Printed October 1976

Sandia Laboratories

SF 2900 Q(7-73)

*When printing a copy of any digitized SAND Report, you are required to update the markings to current standards.*

Issued by Sandia Laboratories, operated for the United States Energy Research & Development Administration by Sandia Corporation.

NOTICE

This report was prepared as an account of work sponsored by the United States Government. Neither the United States nor the United States Energy Research & Development Administration, nor any of their employees, nor any of their contractors, subcontractors, or their employees, makes any warranty, express or implied, or assumes any legal liability or responsibility for the accuracy, completeness or usefulness of any information, apparatus, product or process disclosed, or represents that its use would not infringe privately owned rights.

SF 1004-DF (3-75)

Printed in the United States of America
Available from
National Technical Information Service
U. S. Department of Commerce
5285 Port Royal Road
Springfield, VA 22151
Price: Printed Copy $5.00; Microfiche $2.25.

SAND-76-0527
Unlimited Release
Printed October 1976

# A TWO-DIMENSIONAL VISCOELASTIC MODEL FOR USE IN FINITE DIFFERENCE CALCULATIONS

J. W. Swegle
Computational Physics & Mechanics Division I - 5162
Sandia Laboratories, Albuquerque, New Mexico 87115

## ABSTRACT

A general phenomenological model is developed to describe rate-dependent behavior in multi-dimensional strain. It is applied to the specific problem of two-dimensional viscoelasticity. Results are compared to one-dimensional calculations and to two-dimensional experiments. Calculations are also done for the problems of applied pressures at the surfaces of cylindrical and spherical cavities in viscoelastic media.

## I. Introduction

Recent developments have indicated the need for a calculational model capable of describing strain rate effects in problems involving multi-dimensional strain [1]. Models exist which are suitable for uniaxial strain calculations [2], but a theoretical basis for the general extension of these models into two or more dimensions with substantiating experimental evidence does not exist at this time. A general, coherent, multi-dimensional theory will ultimately be required. However, a first step in this direction, which would also satisfy present calculational needs, would be an easy-to-implement phenomenological model capable of producing the required type of rate sensitive behavior. Problems of immediate interest require a model capable of describing two-dimensional viscoelasticity which would allow comparison to one-dimensional calculations and to experiment [1]. Such a model would be a significant addition to present calculational capabilities.

This paper describes the inclusion in the two-dimensional Lagrangian finite-difference code TOODY [3] of a general phenomenological model which can be used to describe strain rate effects in two or three dimensions. It has previously been successfully used to include stress relaxation due to dislocation theory in a two-dimensional Lagrangian finite-difference code [4]. The method is quite straightforward and easy to include in a finite-difference code, and is capable of describing various types of effects.

## II. Phenomenological Model

### II.1 One-Dimensional Model

The one-dimensional model [2] is based on the equation

$$\dot{\sigma} - F\,(\sigma,\eta)\,\dot{\eta} + G\,(\sigma,\eta) = 0 \qquad (1)$$

where $\sigma$ is the stress in the direction of motion, $\eta$ is the strain, given by

$$\eta = 1 - \rho_o/\rho \tag{2}$$

where $\rho$ is the density, and F and G are arbitrary functions of stress and strain. The form of F for this viscoelastic model is

$$F = F_o\,(1 + F_1\,\eta + F_2\,\eta^2) \tag{3}$$

where

$$F_o = \rho_o\,C_{oi}^{\;2} \tag{4}$$

and $C_{oi}$ is the instantaneous sound speed in the reference state. G is given by

$$G = \frac{\sigma - \sigma_{eq}}{\tau} \tag{5}$$

where

$$\sigma_{eq} = K_o\eta\,(1 + K_1\eta + K_2\eta^2) \tag{6}$$

$$K_o = \rho_o\,C_{oe}^{\;2} \tag{7}$$

and $C_{oe}$ is the equilibrium sound speed in the reference state. $\tau$ is a relaxation time given by

$$\tau = \tau_\ell - g\,(\tau_\ell - \tau_s) \tag{8}$$

where

$$\begin{aligned} g &= 0 && R < 0 \\ g &= [1 - \cos \pi R/R_w]/2 && 0 < R < R_w, \\ g &= 1 && R > R_w, \end{aligned} \tag{9}$$

$$R = \dot{\rho}/\rho \tag{10}$$

and $\tau_\ell$, $\tau_s$ and $R_w$ are adjustable parameters.

II.2. Two-Dimensional Model

The two-dimensional model is based on the equation

$$\dot{S}_{ij} = 2\mu\dot{e}_{ij} - 2\mu F_{ij} \tag{11}$$

where S and e are the stress and strain deviators, $\mu$ is the shear modulus and the $F_{ij}$ are the relaxation functions. This can be derived on the basis of elastic-plastic theory, but is essentially the deviatoric Hooke's law equation with the deviatoric stresses reduced by an arbitrary relaxation function. The implementation of this equation as it stands is made difficult by the necessity of choosing the appropriate forms for the $F_{ij}$. A method for doing this in the general case is not clear.

The model is implemented by extending the procedure used to perform elastic-perfectly-plastic calculations based on Eq. (11). The state of an elastic-perfectly-plastic material may be represented by a point in principal stress deviator space, in which the axes are the principal stress deviators $S_1$, $S_2$, and $S_3$. The Von-Mises yield criterion,

$$J_2 = 1/2\ S_{ij}\ S_{ij} \leq \frac{Y_o^2}{3} \tag{12}$$

where $Y_o$ is the yield strength in simple tension and $J_2$ is the second invariant of the stress deviator tensor, defines a sphere centered on the origin in this space. The requirement that the trace of the stress deviator tensor vanish forces the state point to lie on a plane passing through the origin. The intersection of the Von-Mises sphere with this plane is the circle of Figure 1. Points within the circle are elastic states, and points outside the circle

are plastic states. Elastic-perfectly-plastic theory is implemented by calculating the state of the material from the perfectly elastic equation

$$\dot{S}_{ij} = 2\mu\dot{e}_{ij} \quad . \tag{13}$$

If the state follows a given path and at some time step reaches a state outside the yield surface (e.g., path OA in Fig. 1), it is set normally back to the yield surface to state B, so that Eq. (12) is not violated.

Strain rate sensitive behavior can be modeled by setting the state point only part of the way back to the yield surface during a given time step. Thus the relaxed state of the material during the given time step is represented by point C. The type of behavior to be modeled is determined by the position of the yield surface and the amount of relaxation allowed during a given time step. If the state A of the material calculated from Eq. (13) represents a value of the second invariant of the stress deviator tensor of $J_2$, and that of the relaxed state at C is $J_{2R}$, then

$$J_{2R} = J_2 - F \tag{14}$$

where F may be termed the relaxation function and may be a function of whatever parameters desired. In terms of the individual stress deviators, $J_{2R}$ is obtained by multiplying each principal stress deviator by

$$C = \sqrt{\frac{J_{2R}}{J_2}} = \sqrt{1 - F/J_2} \tag{15}$$

so that the new value of the second invariant of the stress deviator tensor is $J_{2R}$. It is not necessary to calculate the principal stress deviators in order to do this. Since the principal stress deviators are linear functions of the stress deviators in any other reference frame, the same result is obtained by multiplying all stress deviators in any frame by the constant in Eq. (15).

## II.3. Connection of the One- and Two-Dimensional Models

In order to make a connection between this model and that of Eq. (1), the constants for this model have to be chosen to produce the same behavior as the one-dimensional model. The one-dimensional model is described in terms of instantaneous and equilibrium behavior, with the two connected by a relaxation function. The two-dimensional model is described in terms of the elastic states given by Eq. (13) which relax back to states on the yield surface. Thus the material is described elastically before any relaxation takes place, and this corresponds to the instantaneous behavior of the one-dimensional model. The equilibrium behavior corresponds to the fully relaxed states on the yield surface. To correspond to the relaxation function of Eq. (5), F of Eq. (14) is taken as

$$F = \frac{J_2 - J_{2eq}}{\tau} \Delta t \tag{16}$$

where $\Delta t$ is the time step and $\tau$ is given by Eqs. (8), (9) and (10). The equilibrium behavior is modeled by taking a zero radius yield surface so that the equilibrium response is hydrodynamic with the pressure given by

$$P = K_o \eta \, (1 + K_1 \eta + K_2 \eta^2) \tag{17}$$

with $K_o$, $K_1$, and $K_2$ the same constants used in Eq. (6). The only parameter to vary in Eq. (13) is $\mu$, and this has to be related to the instantaneous response given by Eq. (3). Since F is $\rho C_1^2$ where $C_1$ is the instantaneous sound speed, the constants can be related by the equation

$$C_o^2 = C_\ell^2 - 4/3 \, C_s^2 \tag{18}$$

where $C_o$ is the bulk sound speed corresponding to $C_{oe}$ and given by

$$C_o^2 = (\partial P/\partial \rho)_s \, , \tag{19}$$

$C_\ell$ is the longitudinal sound speed corresponding to $C_i$, and $C_s$ is the shear wave sound speed given by $(\mu/\rho)^{\frac{1}{2}}$. Solving Eq. (18) for $\mu$ yields

$$\mu = 3/4\ \rho \left[\frac{f_o}{\rho}\ (1 + f_1\eta + f_2\eta^2) - \rho_o/\rho^2 K_o\ (1 + 2K_1\eta + 3K_2\eta^2)\right] \tag{20}$$

with Eqs. (17) and (19) used to evaluate $C_o^2$. Assuming $\mu$ to be of the form

$$\mu = \mu_o\ (1 + \mu_1\eta + \mu_2\eta^2 + \mu_3\eta^3) \tag{21}$$

and equating coefficients of powers of $\eta$ yields

$$\begin{aligned} \mu_o &= 3/4\ (f_o - K_o)\ , \\ \mu_1 &= \frac{f_o f_1 - 2K_o K_1 + K_o}{f_o - K_o}\ , \\ \mu_2 &= \frac{f_o f_2 - 3K_o K_2 + 2K_o K_1}{f_o - K_o}\ , \text{ and} \\ \mu_3 &= \frac{3K_o K_2}{f_o - K_o}\ . \end{aligned} \tag{22}$$

Since $\mu_o$ and $K_o$ are related by

$$\mu_o = \frac{3(1 - 2\nu)}{2(1 + \nu)}\ K_o \tag{23}$$

where $\nu$ is Poisson's ratio, $\nu$ is given by

$$\nu = \frac{3K_o - 2\mu_o}{2\mu_o + 6K_o}\ . \tag{24}$$

This defines all material properties needed to implement the model. Since $J_{2eq}$ is assumed to be zero, the only extra calculation necessary is to multiply each stress deviator at each time step by

$$C = \left\{ \max\left(0,\ 1 - \frac{\Delta t}{\tau}\right) \right\}^{\frac{1}{2}} . \tag{25}$$

## III. Uniaxial Strain Calculations

In order to evaluate the two-dimensional viscoelastic model, comparisons were made to WONDY [5] runs using the one-dimensional viscoelastic model. The calculations were made for the problem of the impact of a $Al_2O_3$-epoxy flyer upon a similar target backed by fused quartz [1]. The calculated variable of primary interest was the velocity history in the target at the interface between the $Al_2O_3$-epoxy and the fused quartz. This was compared to laser interferometer records of the experiment obtained by Munson et. al. [1]. The relaxation time $\tau$ given in Eqs. (8), (9) and (10) was chosen to match previous [1] experimental observations for the $Al_2O_3$-epoxy mixtures which showed release wave velocities to be larger than unloading wave velocities. Thus a two-rate relaxation time with long relaxation times on unloading and short relaxation times on loading was used in the one-dimensional model. The identical form with the same constants was used in the two-dimensional model, even though it is not clear that identical constants $\tau$ should produce identical relaxation rates in the two different models.

Fig. 2 shows the results for a 6.28 mm flyer with a velocity of .27 mm/μs impacting a 6.34 mm thick target. The constants used in the equations for $\tau$ were .25 μs for $\tau_\ell$, .02 μs for $\tau_s$ and .11 μs for $R_w$. The dotted line is the experimental result and the solid line is the calculated result obtained by Munson et. al. [1].

Figures 3, 4, 5 and 6 show TOODY calculations for the same problem using the two-dimensional viscoelastic model compared to the one-dimensional results. These calculations were done using material properties derived from those of the one-dimensional model as described in Section II.2. Figure 3 shows the wave profile when the material is always hydrodynamic, which means the material

response is along the equilibrium curve. This corresponds to the case $\tau = 0$. Fig. 4 shows the wave profile when the material is always elastic, so that the instantaneous response is always seen. This corresponds to the case $\tau = \infty$. Fig. 5 shows the viscoelastic response with all parameters the same as in the one-dimensional model, and Fig. 6 shows the result of changing the value of $\tau_\ell$ to .1 μs. The curve calculated using $\tau_\ell$ = .1 μs in the two-dimensional viscoelastic model shows excellent agreement with the WONDY results, but the $\tau_\ell$ = .25 μs calculation seems to give better agreement with the release portion of the experimental wave profile. Thus the two-dimensional model can very accurately reproduce the results of WONDY calculations using the viscoelastic constitutive relation, although the relaxation time constants are slightly different. This is attributed to differences in the relaxation methods in the one- and two-dimensional models.

## IV. Cylindrical and Spherical Calculations

A further test of the two-dimensional model was accomplished by predicting the results of configurations in which a pressure is applied to the boundary of cylindrical or spherical cavities in a material medium. Analytic solutions are available for the case of completely elastic material response [6], and the results of the viscoelastic calculations can be compared to these solutions. An analytic solution is not available for the viscoelastic case, so a rigorous evaluation of the results of these calculations requires comparison to experiment. Although these problems involve one-dimensional motion in the radial direction, they cannot presently be performed on WONDY because the WONDY viscoelastic model is limited to uniaxial strain.

Figs. 7, 8, 9 and 10 show the analytically calculated response of a medium subjected to a constant pressure of 0.6 GPa at the boundary of a 5.0 mm radius spherical cavity. Figs. 7 and 8 show the circumferential stress and radial

velocity as a function of radius at several times for a hydrodynamic material. Figs. 9 and 10 show the same quantities for an elastic material. Results for cylindrical cavities are qualitatively similar. The most interesting feature of these calculations is the major difference between the response of the hydrodynamic and elastic materials. In the elastic material the circumferential stresses are compressional at the head of the wave, but tension quickly follows. The radial velocity is a maximum at the wave front and quickly drops off to negative values. The hydrodynamic material shows a response that is almost opposite in character. The circumferential stresses are always compressional and the radial velocity is a minimum at the wave front and increases toward the cavity boundary. Finite difference code calculations for spherical cavities in elastic and hydrodynamic materials are in agreement with these results. Similar calculations for cylindrical cavities show most of the same major features.

Figs. 11 and 12 show the results of finite difference code calculations for the same configuration as in the analytic calculations except that the viscoelastic material model is used. The material properties and relaxation rate are the same as those given in Section III, with $\tau_\ell = .25\ \mu s$. The figures show that with this relaxation rate the wave profiles show the same general features seen in the hydrodynamic analytic calculations. The circumferential stress is compressional and the radial velocity increases rather than decreases with decreasing radius. However, the magnitude and wave shape for the circumferential stress do show significant differences from either the hydrodynamic or elastic cases. Figs. 13 and 14 show the circumferential stress and radial velocity for the problem of a constant 0.6 GPa stress on a 25.0 mm diameter cylindrical cavity in a viscoelastic medium with the same material properties as those used in the elastic calculation. Again, the relaxation rate is such that the material response shows the same general features seen in the hydrodynamic analytic calculations.

These results indicate that the geometries considered here would provide useful configurations for experiments designed to measure material properties. The major differences between the hydrodynamic and elastic responses indicate that these geometries would be worthwhile for experiments designed to detect material strength. The rate of transformation between elastic and hydrodynamic responses should also provide information on viscous and rate effects. Although a means for obtaining quantitative measurements of these quantities is not presently clear, further studies of different cavity radii and relaxation rates should produce further insight into the problem.

## V. Comparison with Two-Dimensional Experimental Data

The final evaluation of the two-dimensional model was to compare its predictions to the results of measurements made of wave profiles in explosively driven ferroelectric power supplies using $Al_2O_3$-epoxy mixtures as an encapsulant. Fig. 15 shows the power supply configuration as zoned by Buller [7]. Laser interferometer velocity measurements were made by Schuler [8] at the quartz-potting compound interface for two different thicknesses of $Al_2O_3$ potting material.

Figs. 16 and 17 show the calculated wave profiles for the thin and thick experiments respectively, obtained by assuming that the potting compound is hydrodynamic, compared to the experimental records. There is a significant discrepancy between the calculated and measured results. The calculated results show a two-peak structure which is absent in the experimental results, and the calculated velocity maximum is too high by a factor of 3 for the thick configuration.

Figs. 18 and 19 show the calculated results using the two-dimensional viscoelastic model for the potting compound with $\tau_\ell = .25$ μs. These results are in much better agreement with experiment. The two-peak structure is

missing from the calculation for the thicker configuration so that the release wave profile is in agreement with experiment, and the peak velocity is .166 mm/μs as compared to .135 mm/μs for the experimental record and .37 mm/μs for the calculation without the viscoelastic model. Thus the two-dimensional viscoelastic model is successful in predicting the results of both these two-dimensional experiments.

## VI. Conclusions

The two-dimensional phenomenological viscoelastic model described here has been implemented in a two-dimensional Lagrangian finite-difference code and has been compared to the results of one-dimensional viscoelastic calculations and two-dimensional experiments. It has been shown to be able to reproduce the results of both. Its ease of implementation and versatile capabilities for describing different rate effects by changing the functional dependence of the relaxation function make it a useful tool for studying these effects in various different geometries.

## VII. Acknowledgements

Thanks are due to the following people for their contributions to this paper: Rod Boade for emphasizing the need for the model and providing the model for the relaxation rate; Darrell Munson and Karl Schuler for providing the one-dimensional data; Larry Bertholf for providing the analytic solution for the problem of transient waves from a spherical cavity in an elastic medium; Dan Buller for the original TOODY zoning of the ferroelectric power supplies; and Karl Schuler for the use of unpublished data on the two-dimensional experiments and for many helpful discussions and comments regarding the work.

## References


1. "Stress Wave Propagation in $Al_2O_3$-Epoxy Mixture," D. E. Munson, R. R. Boade, K. W. Schuler, SAND-76-0376, in preparation.

2. "A General Viscoelastic Constitutive Relation for Use in Wave Propagation Calculations," R. J. Lawrence, SC-RR-72-0114, Feb. 1972.

3. "TOODY-II - A Computer Program for Two-Dimensional Wave Propagation," L. D. Bertholf, S. E. Benzley, SC-RR-68-41, Nov. 1968.

4. "A Method for Performing and Interpreting Gas Gun Experiments in Two-Dimensional Strain," J. W. Swegle, Ph.D. Thesis, Washington State University, Pullman, Washington, 1976, p. 144.

5. "WONDY IIIA - A Computer Program for One-Dimensional Wave Propagation," R. J. Lawrence, SC-DR-70-315, August 1970.

6. "Transient Compression Waves from Spherical and Cylindrical Cavities," H. L. Selberg, Arkiv För Fysik, Band 5, nr 7, p. 97 (1951).

7. D. L. Buller, private communication.

8. K. W. Schuler, private communication.

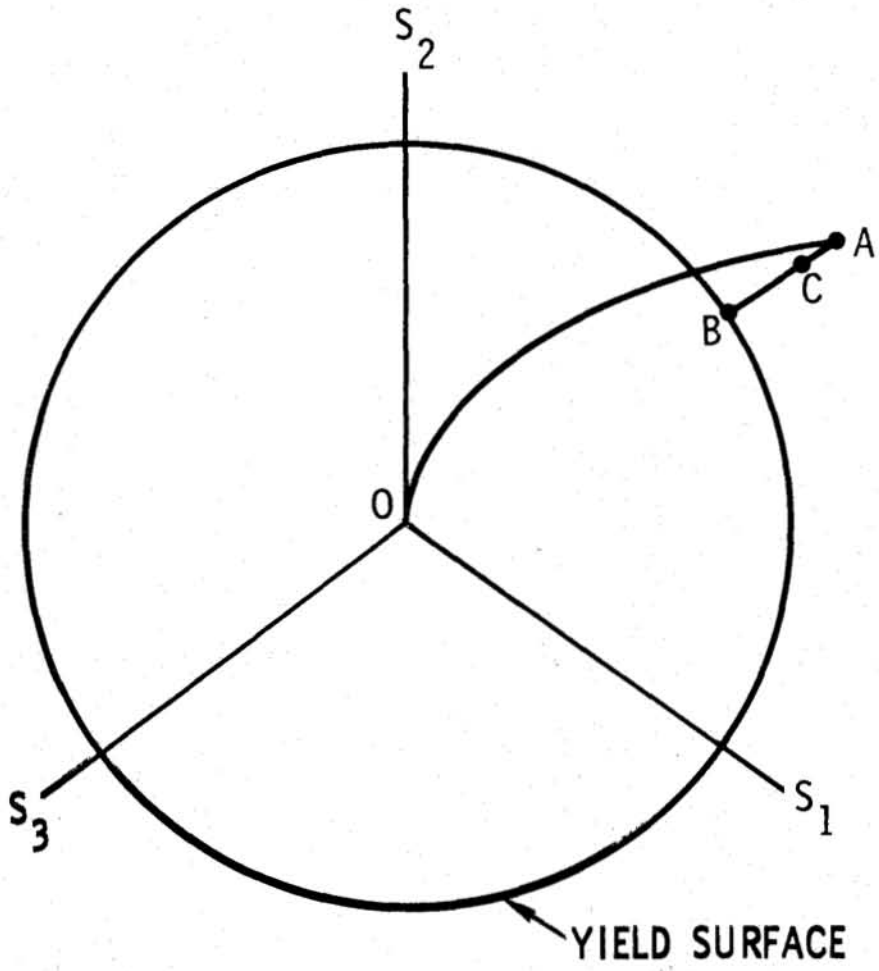


FIG. 1. REPRESENTATION OF MATERIAL STATE POINTS IN PRINCIPAL STRESS DEVIATOR SPACE

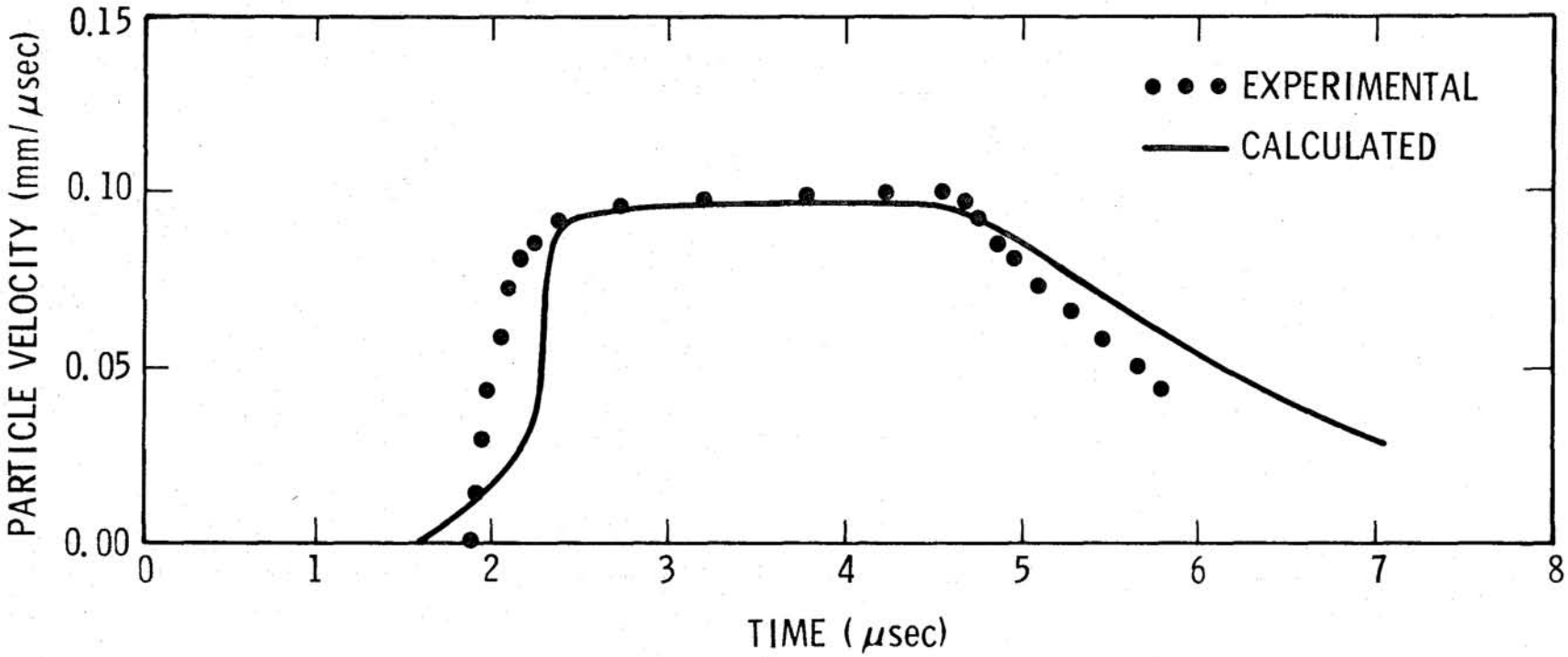


FIG. 2. COMPARISON OF EXPERIMENTAL AND CALCULATED RESULTS FOR THE 1-D VISCOELASTIC MODEL

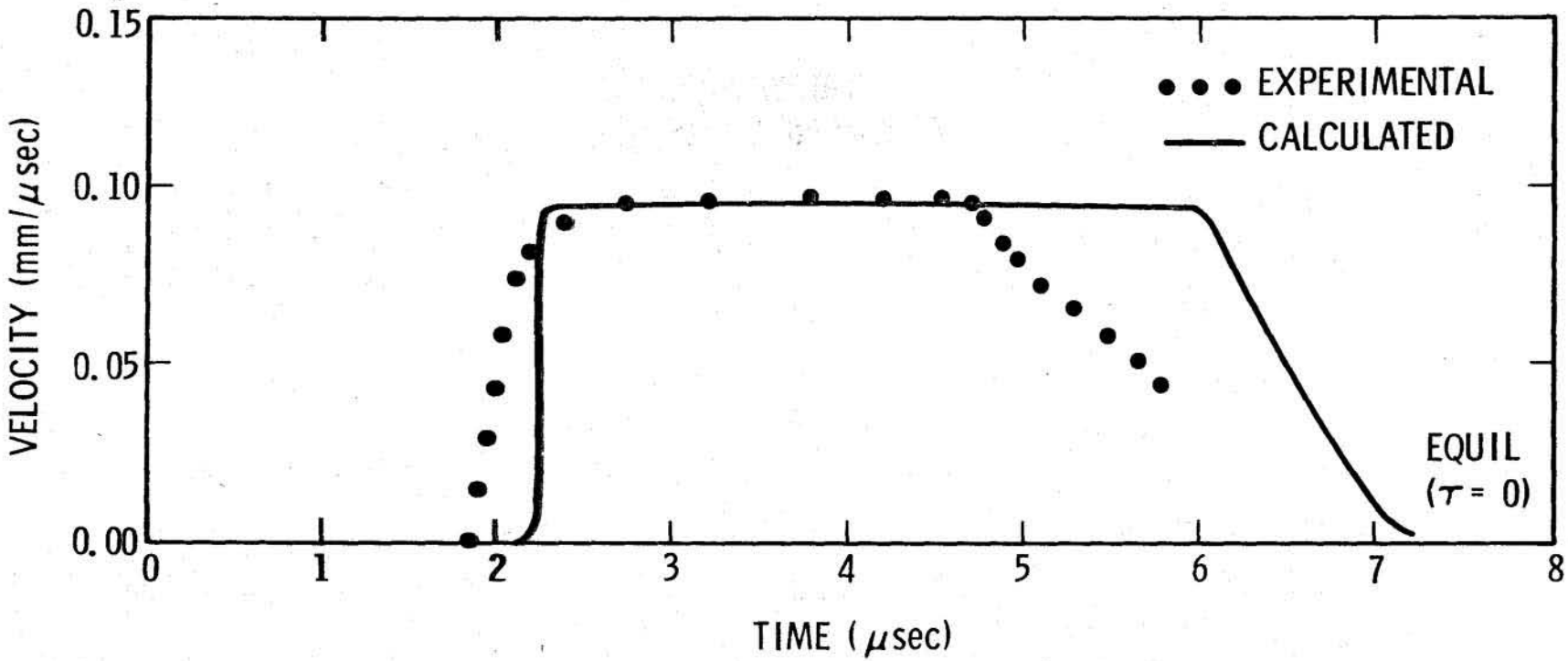


**FIG. 3.** EQUILIBRIUM RESPONSE OF TWO-DIMENSIONAL VISCOELASTIC MODEL

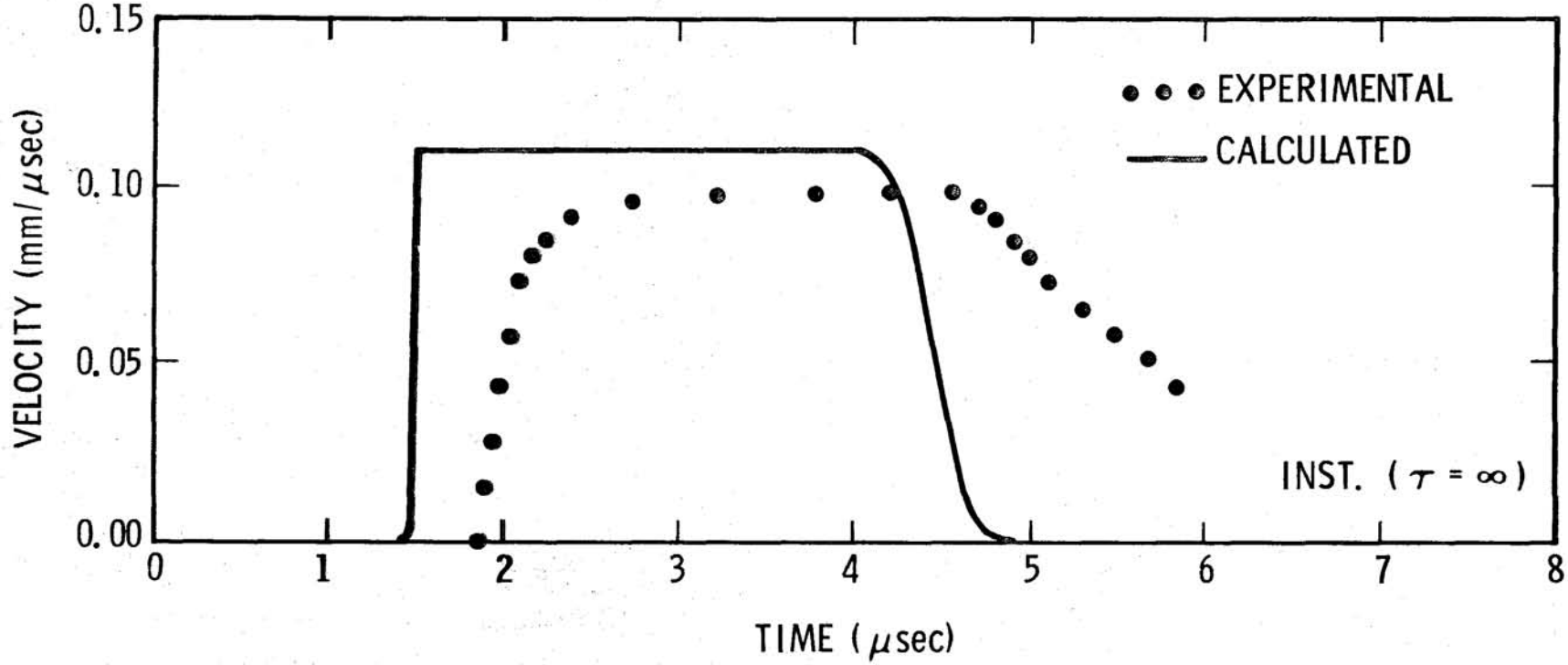


FIG. 4. INSTANTANEOUS RESPONSE OF TWO-DIMENSIONAL VISCOELASTIC MODEL

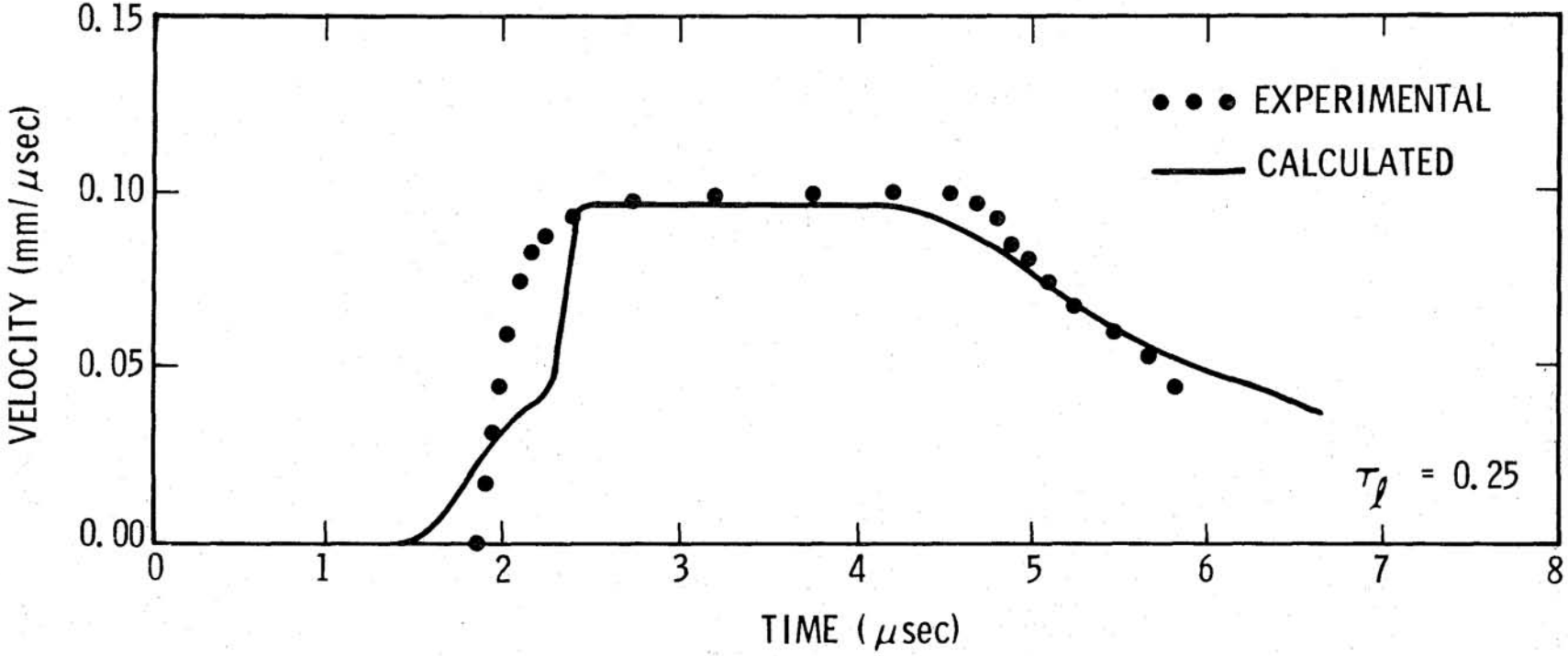


FIG. 5. TWO-DIMENSIONAL VISCOELASTIC MODEL WITH $\tau_\ell$ = 0.25 μsec

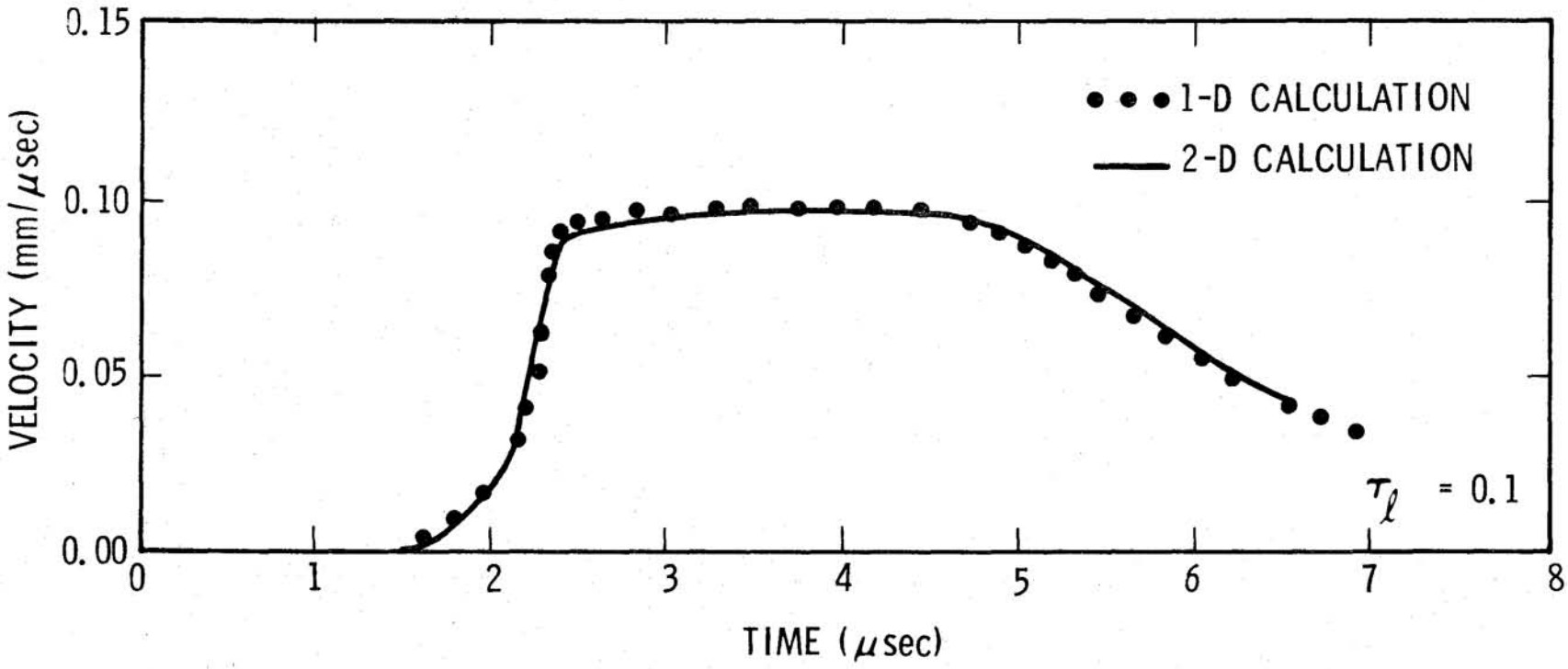


FIG. 6. TWO-DIMENSIONAL VISCOELASTIC MODEL WITH $\tau_\ell$ = 0.1 $\mu$sec

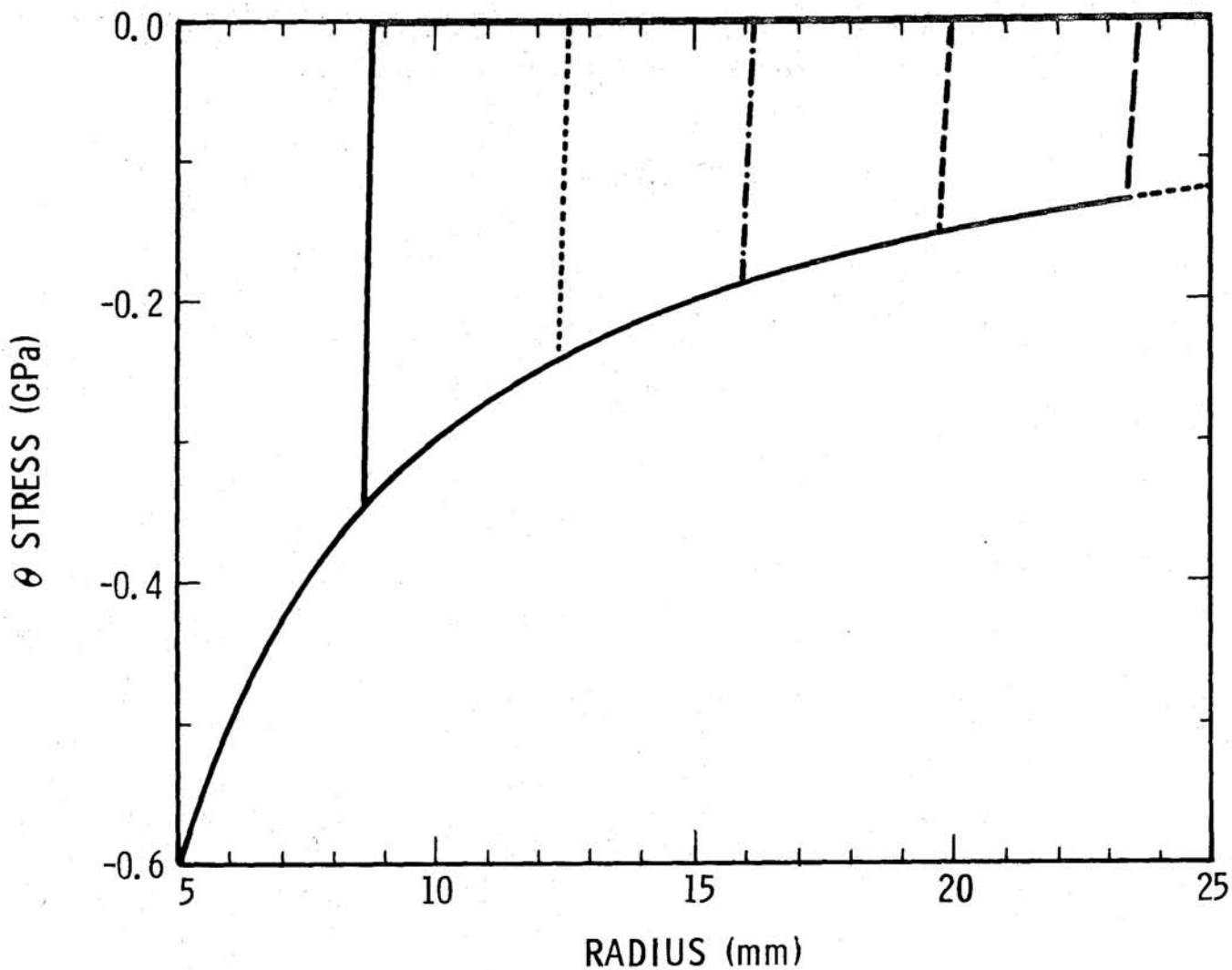


FIG. 7. CIRCUMFERENTIAL STRESS vs RADIUS
HYDRO T = 1.5, 3.0, 4.5, 6.0, 7.5, 9.0 μsec

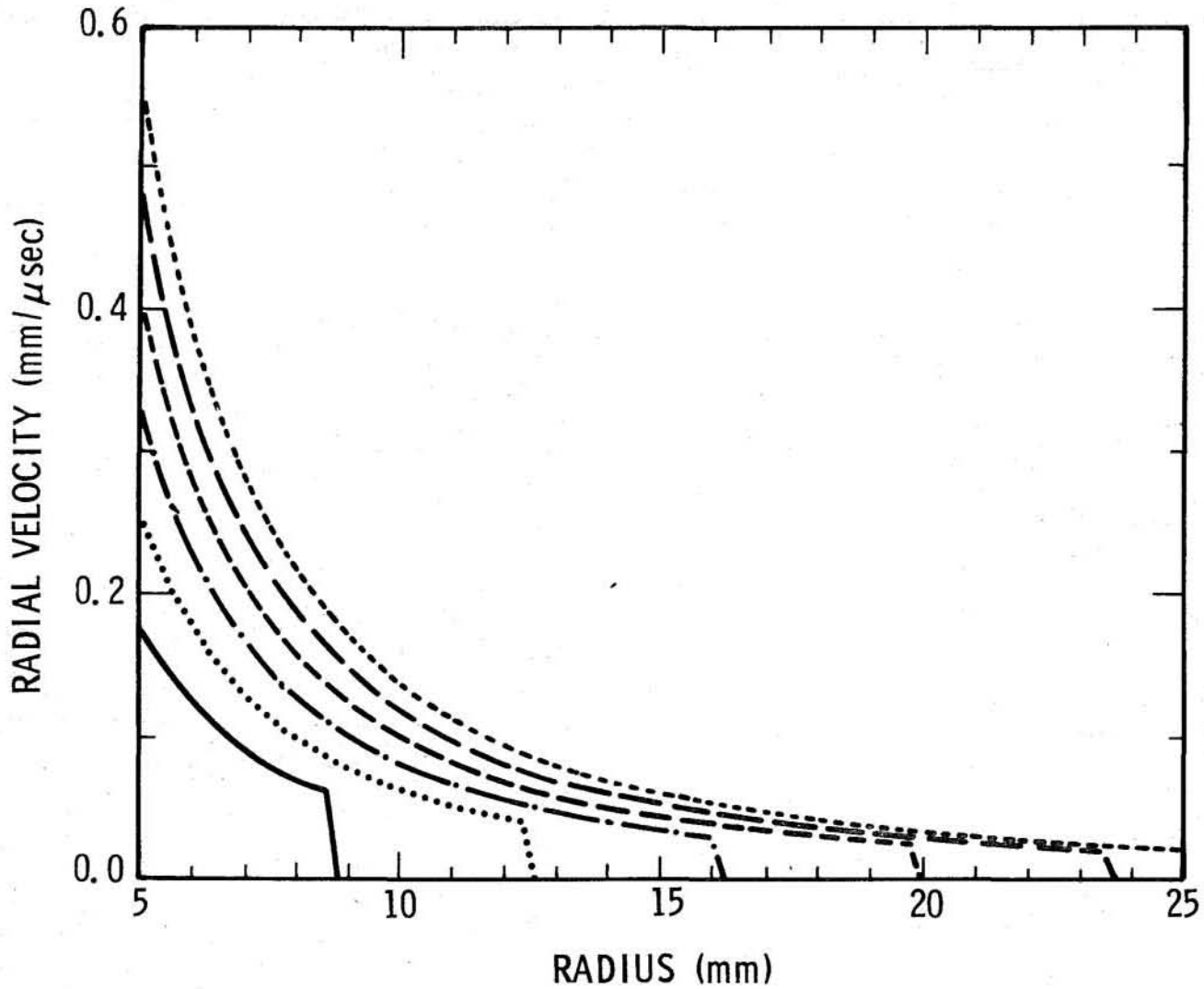


FIG. 8. RADIAL VELOCITY vs RADIUS
HYDRO T = 1.5, 3.0, 4.5, 6.0, 7.5, 9.0 μsec

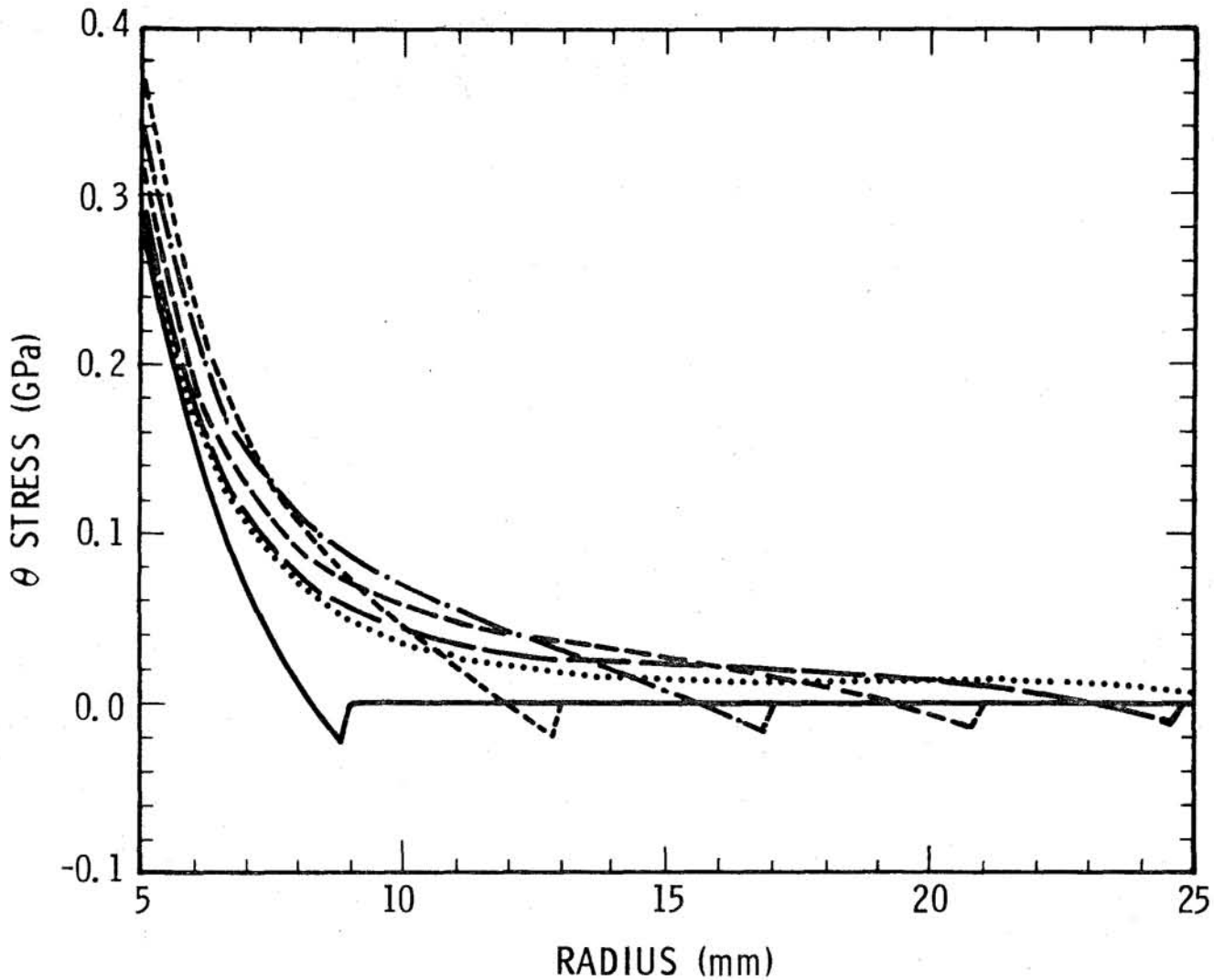


FIG. 9. CIRCUMFERENTIAL STRESS vs RADIUS
ELASTIC T = 1, 2, 3, 4, 5, 6 $\mu$sec

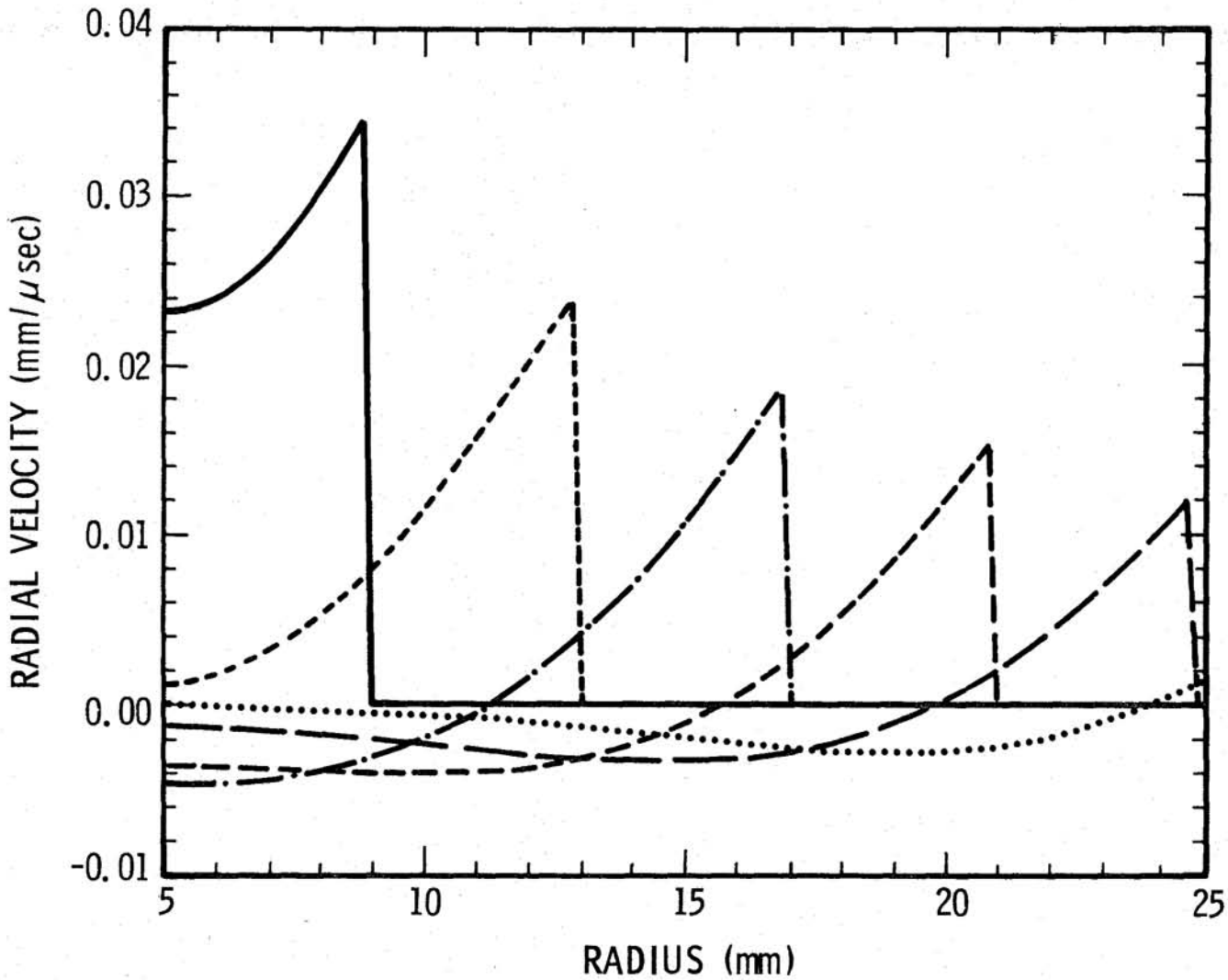


FIG. 10. RADIAL VELOCITY vs RADIUS
ELASTIC T = 1, 2, 3, 4, 5, 6 μsec

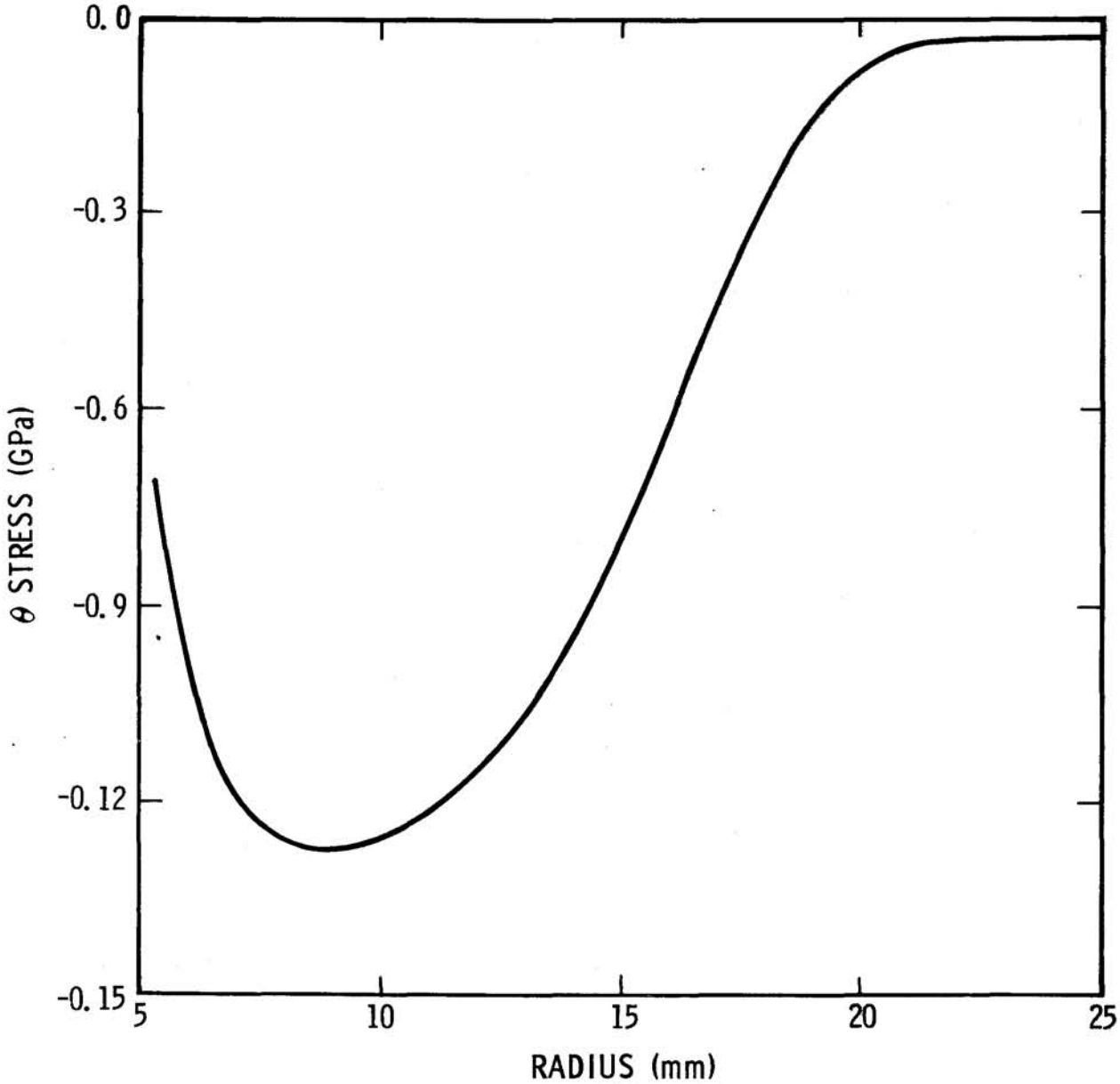


FIG. 11. CIRCUMFERENTIAL STRESS vs RADIUS FOR SPHERICAL CAVITY IN VISCOELASTIC MATERIAL. T = 4.5 $\mu$sec.

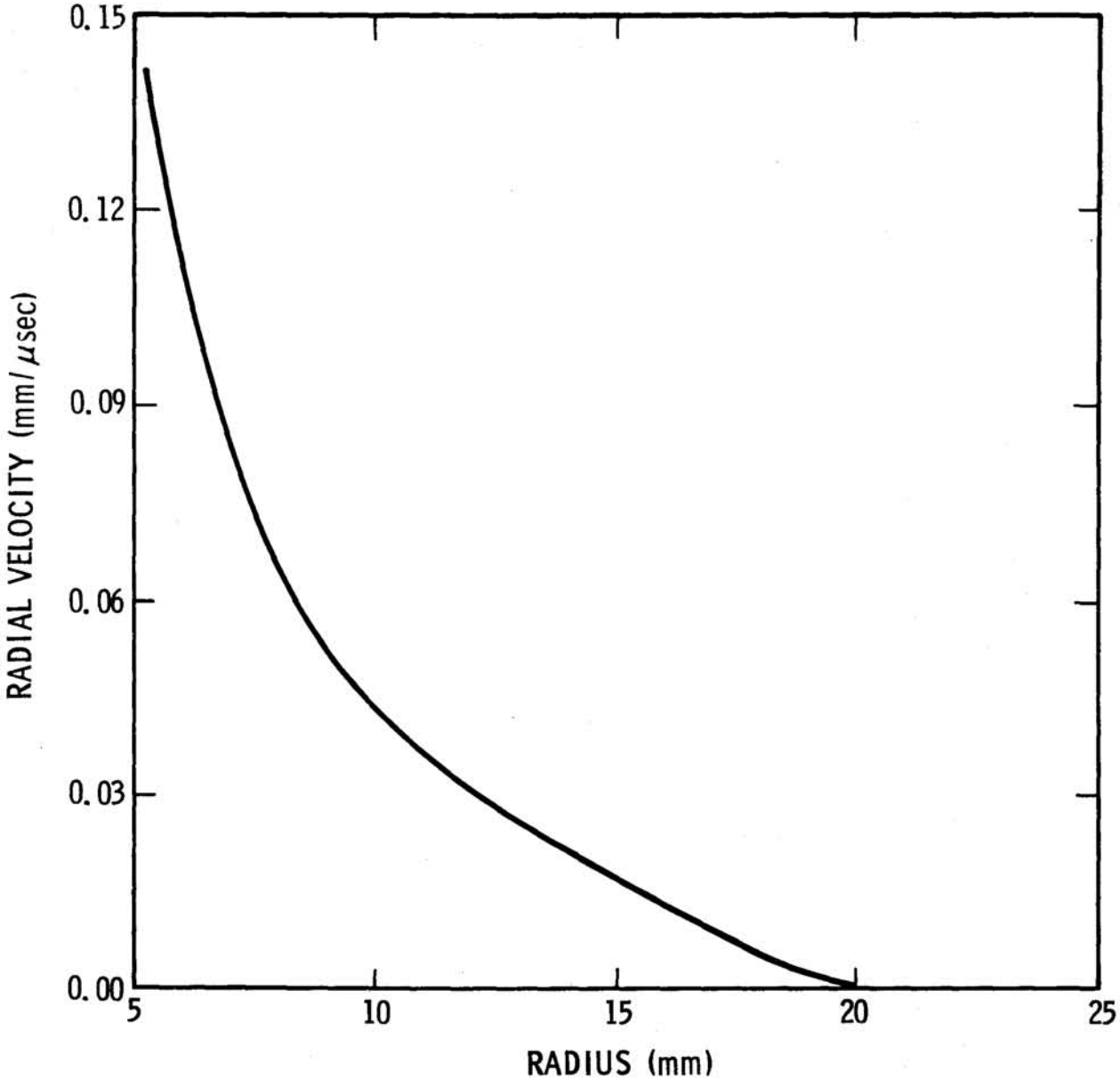


FIG. 12. RADIAL VELOCITY vs RADIUS FOR A SPHERICAL CAVITY IN A VISCOELASTIC MEDIUM. T = 4.5 μsec.

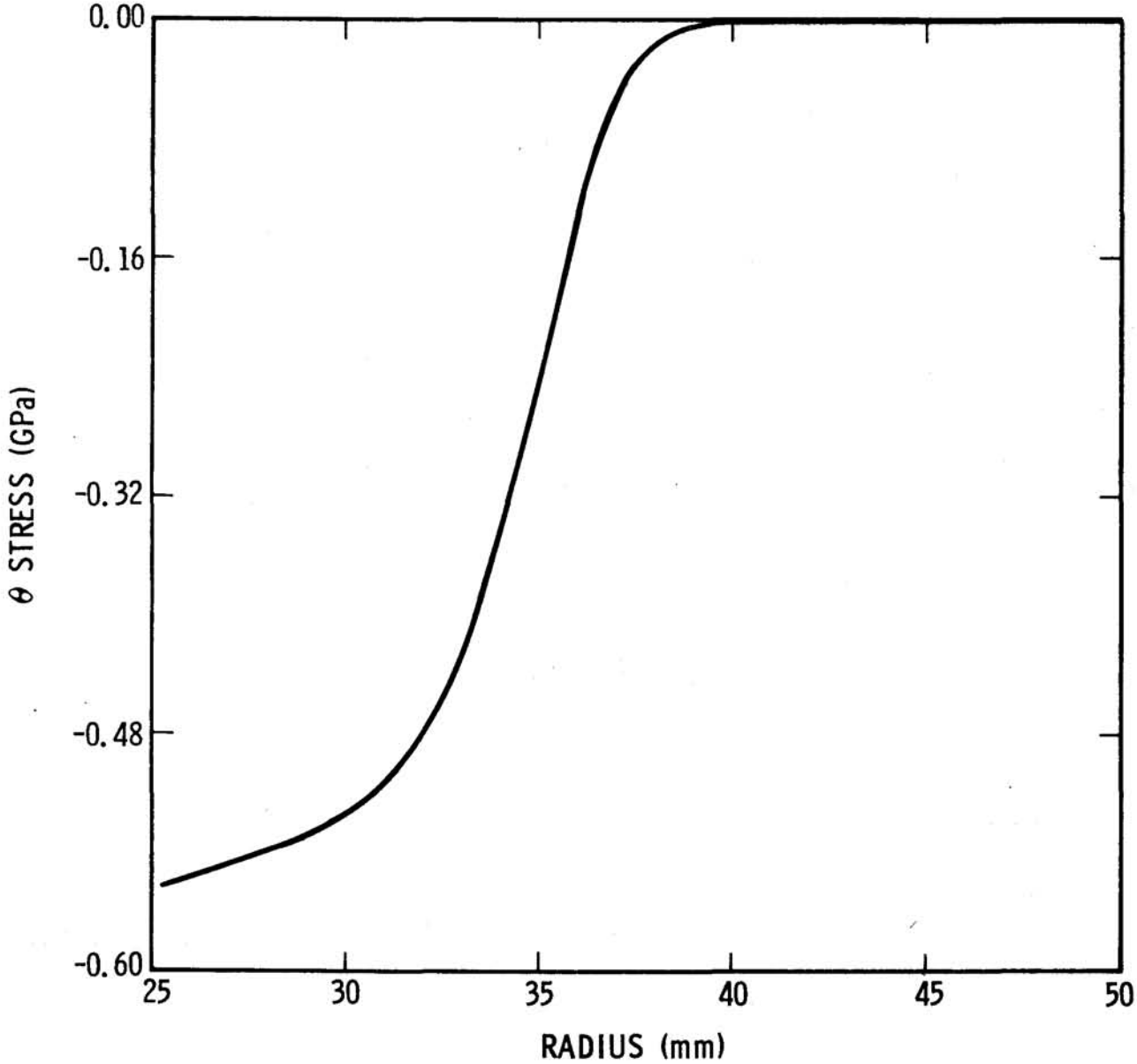


FIG. 13. CIRCUMFERENTIAL STRESS vs RADIUS FOR A CYLINDRICAL CAVITY IN A VISCOELASTIC MEDIUM. T = 4 $\mu$sec.

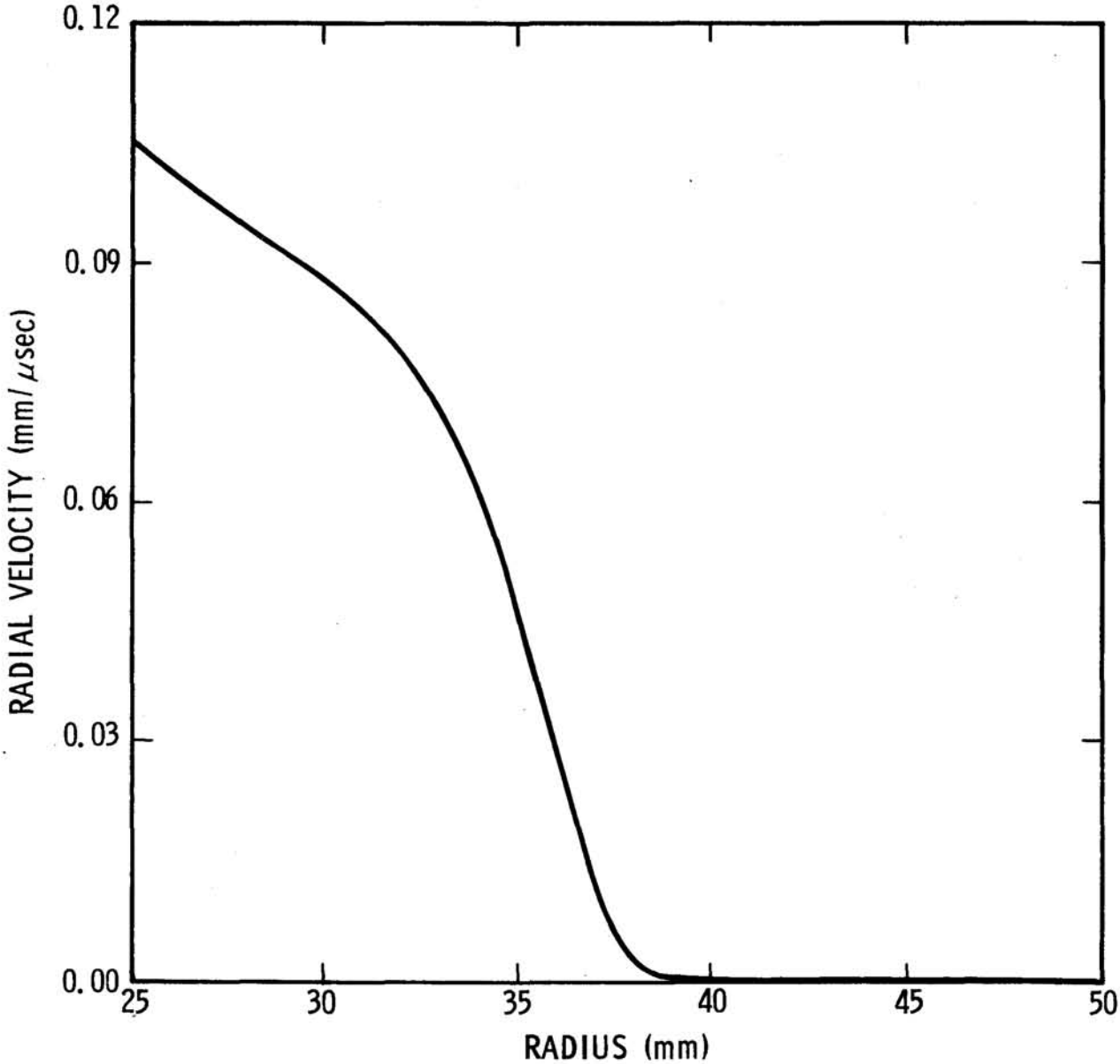


FIG. 14. RADIAL VELOCITY vs RADIUS FOR A CYLINDRICAL CAVITY IN A VISCOELASTIC MEDIUM. T = 4 μsec.

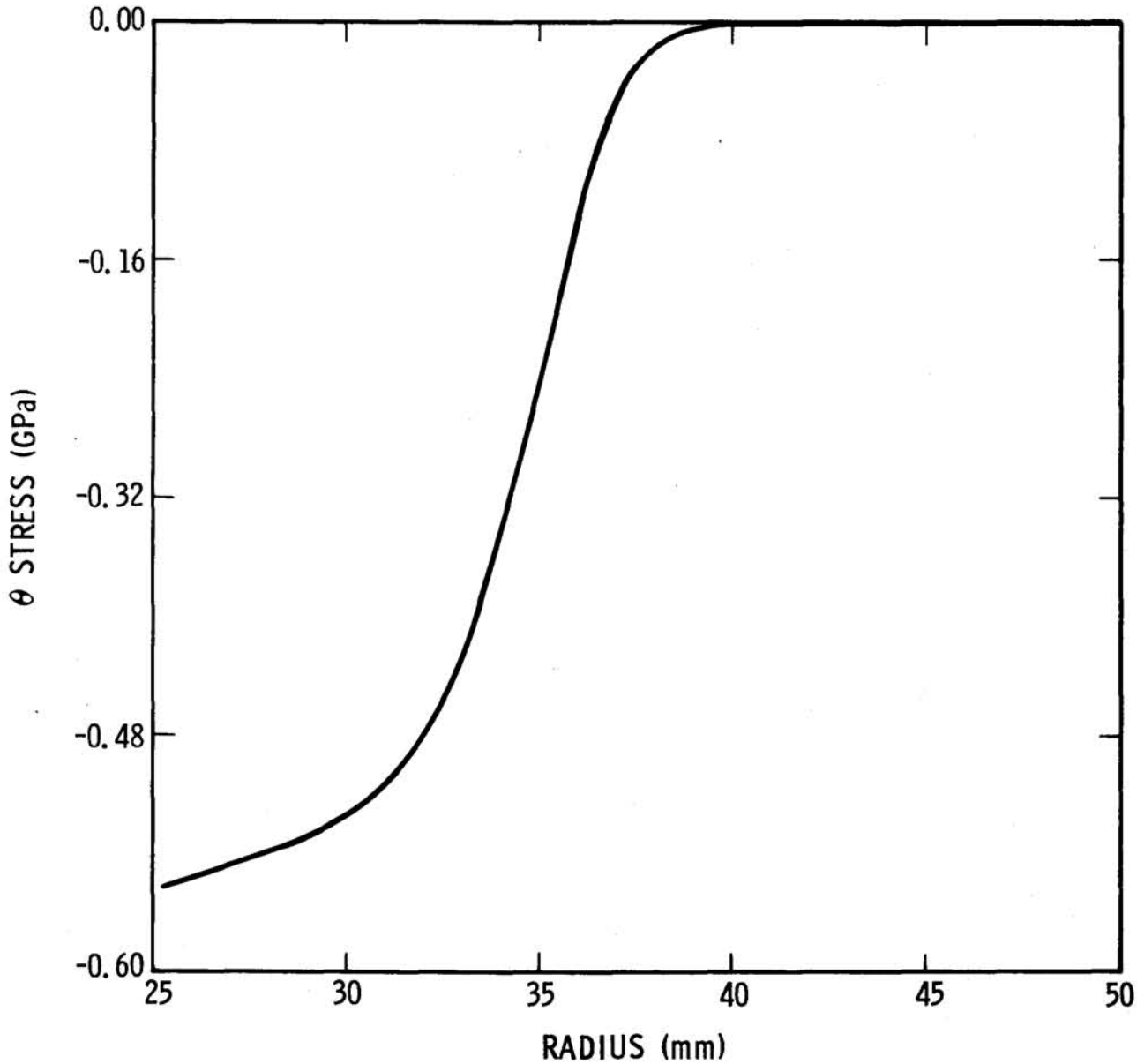


FIG. 13. CIRCUMFERENTIAL STRESS vs RADIUS FOR A CYLINDRICAL CAVITY IN A VISCOELASTIC MEDIUM. T = 4 $\mu$sec.

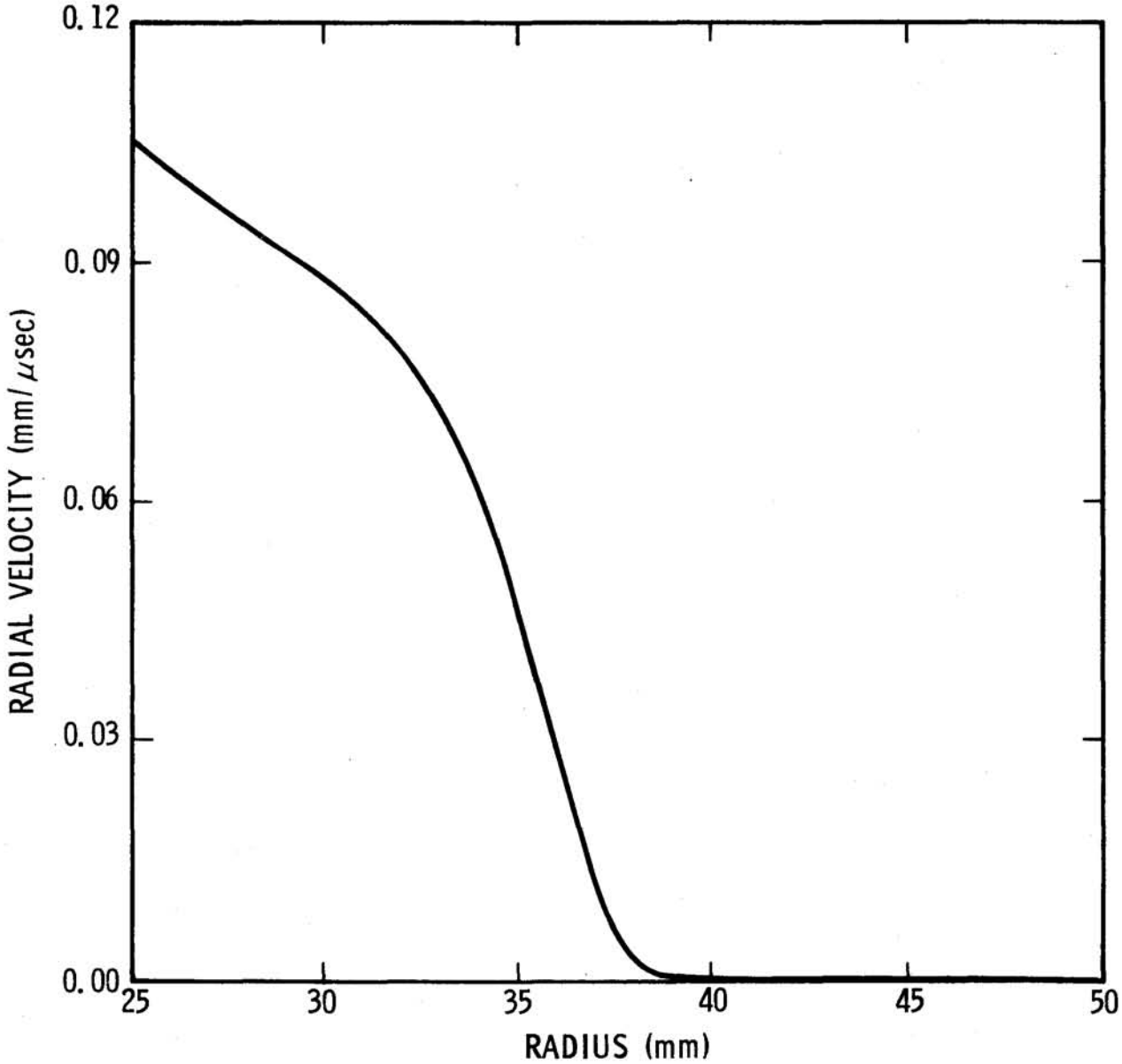


FIG. 14. RADIAL VELOCITY vs RADIUS FOR A CYLINDRICAL CAVITY IN A VISCOELASTIC MEDIUM. T = 4 μsec.

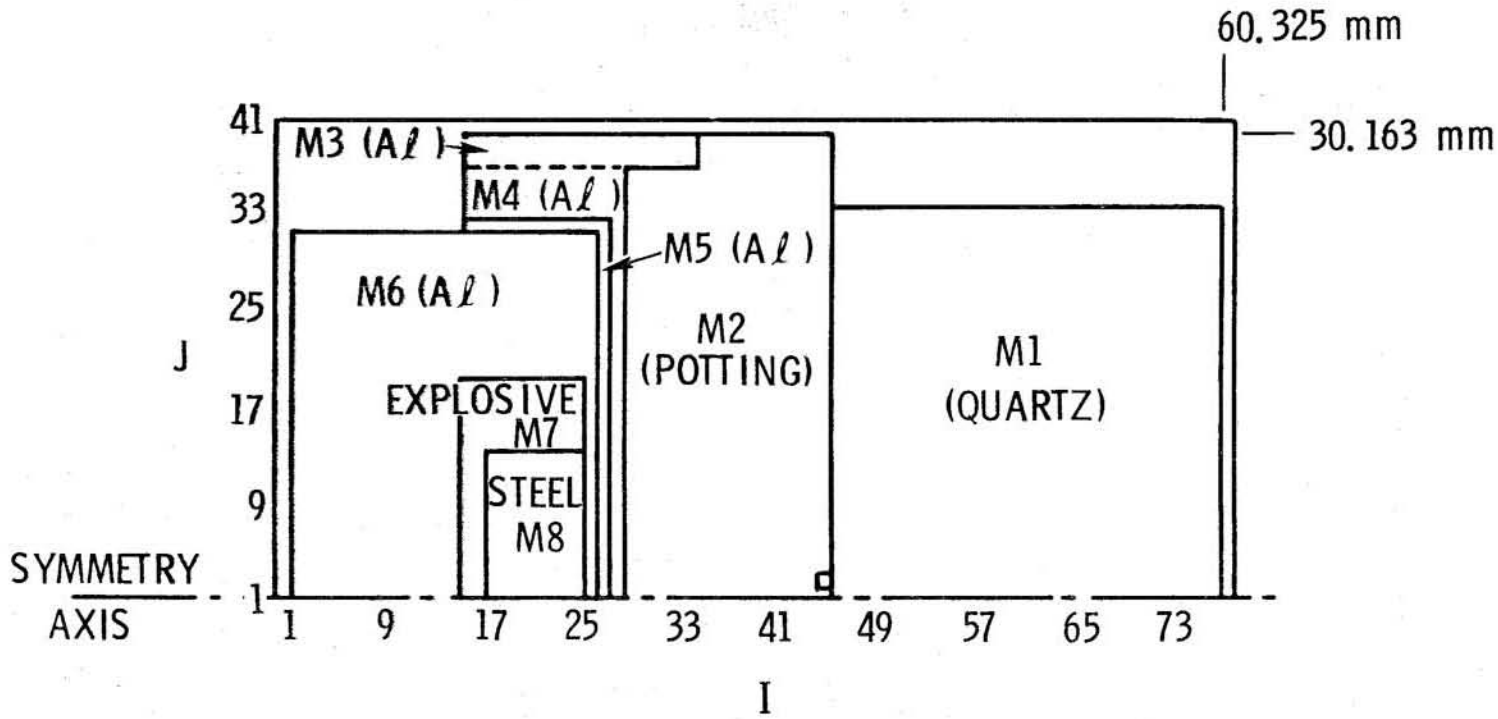


FIG. 15. POWER SUPPLY CONFIGURATION

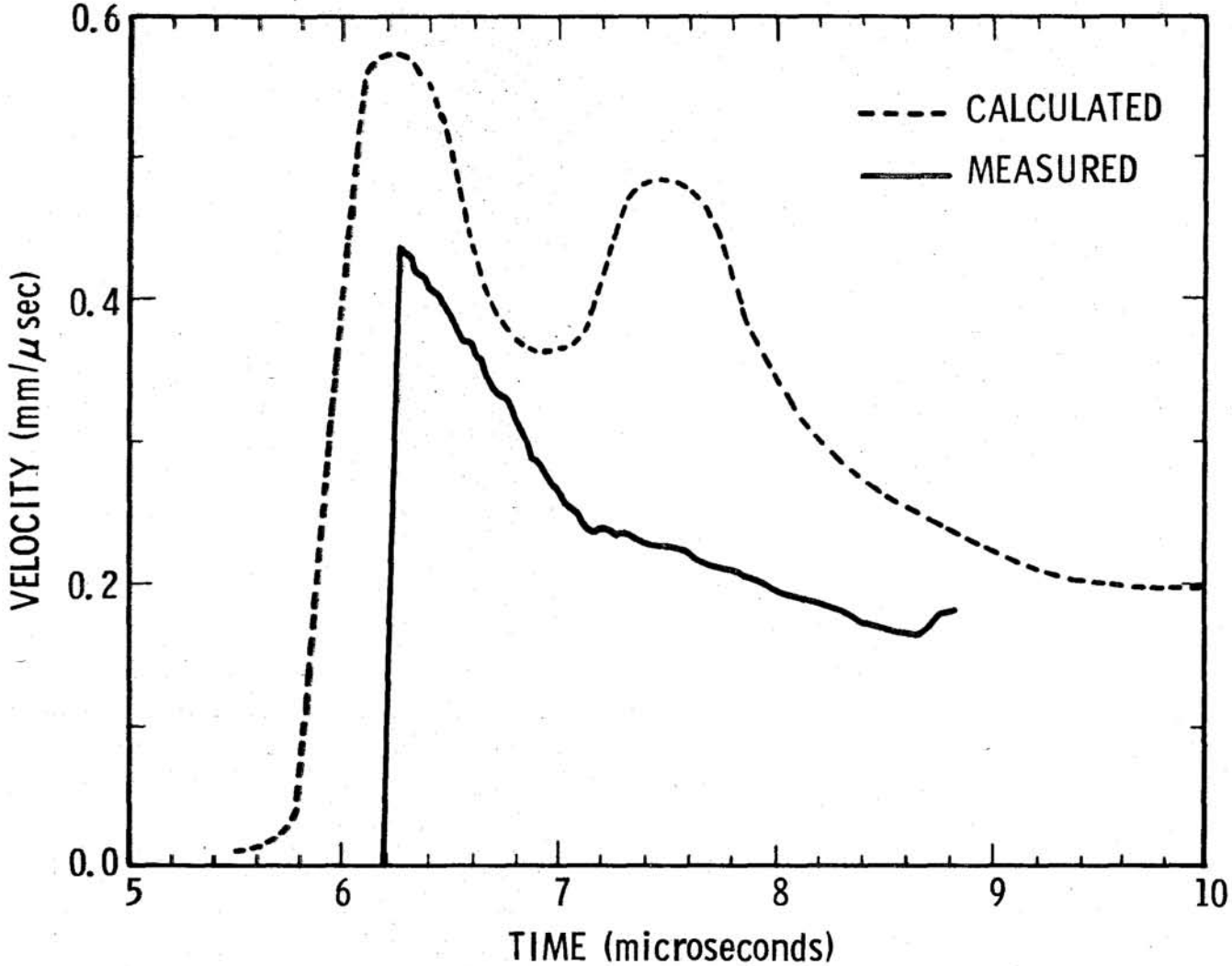


FIG. 16. COMPARISON OF HYDRO CALCULATION TO EXPERIMENTAL RECORD FOR THIN CONFIGURATION

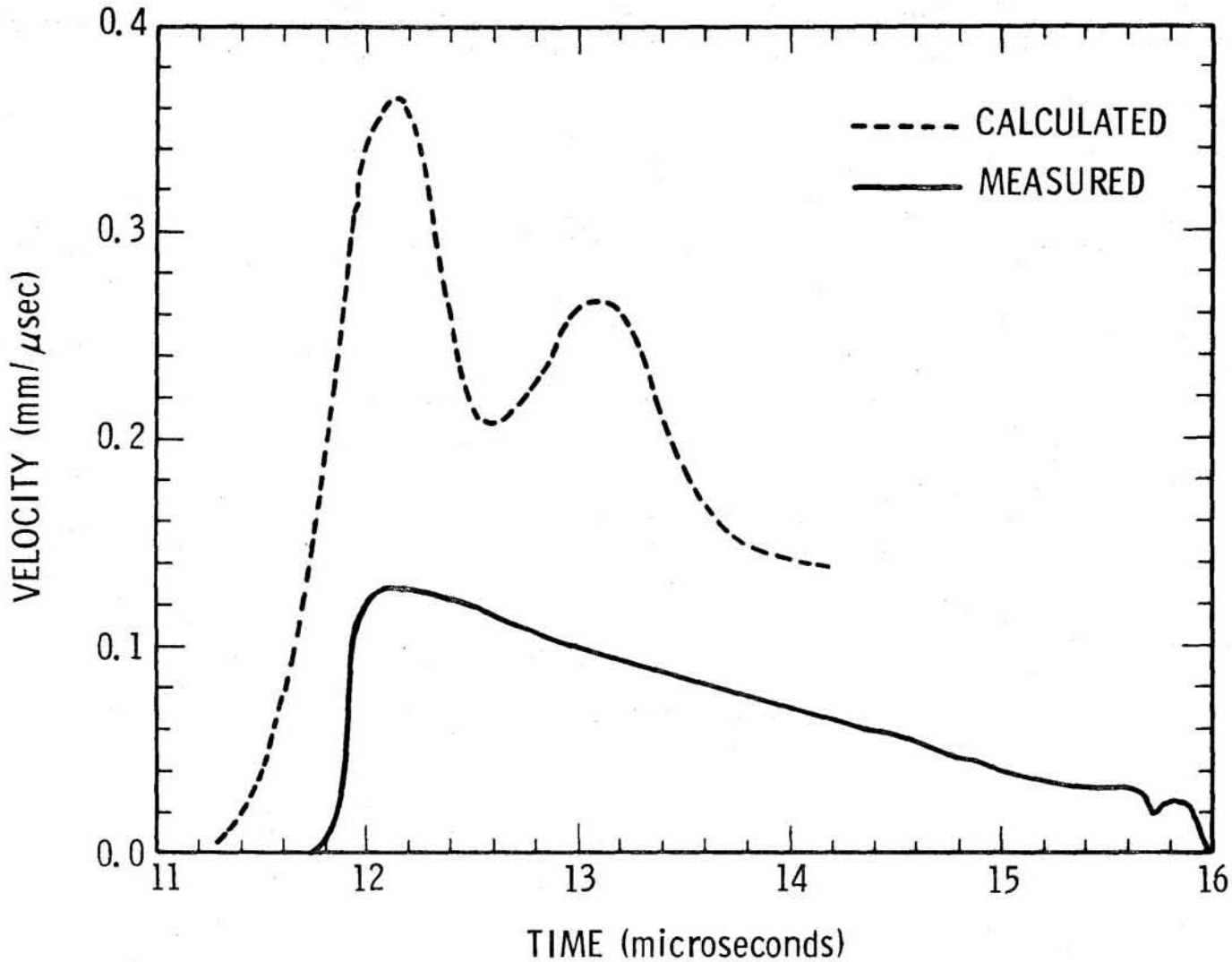


FIG. 17. COMPARISON OF HYDRO CALCULATION TO EXPERIMENTAL RECORD FOR THICK CONFIGURATION

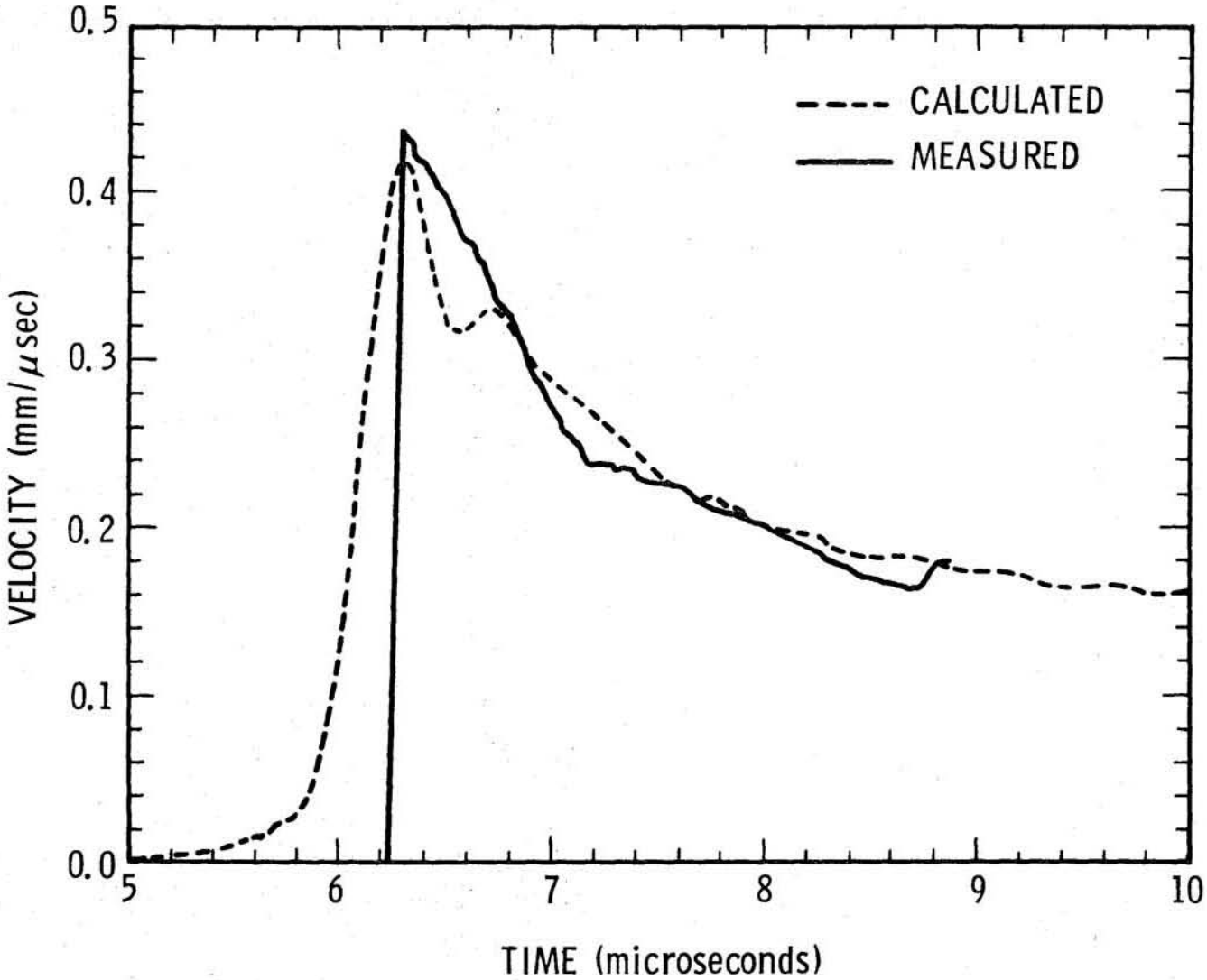


FIG. 18. COMPARISON OF VISCOELASTIC CALCULATION TO EXPERIMENTAL RECORD FOR THIN CONFIGURATION

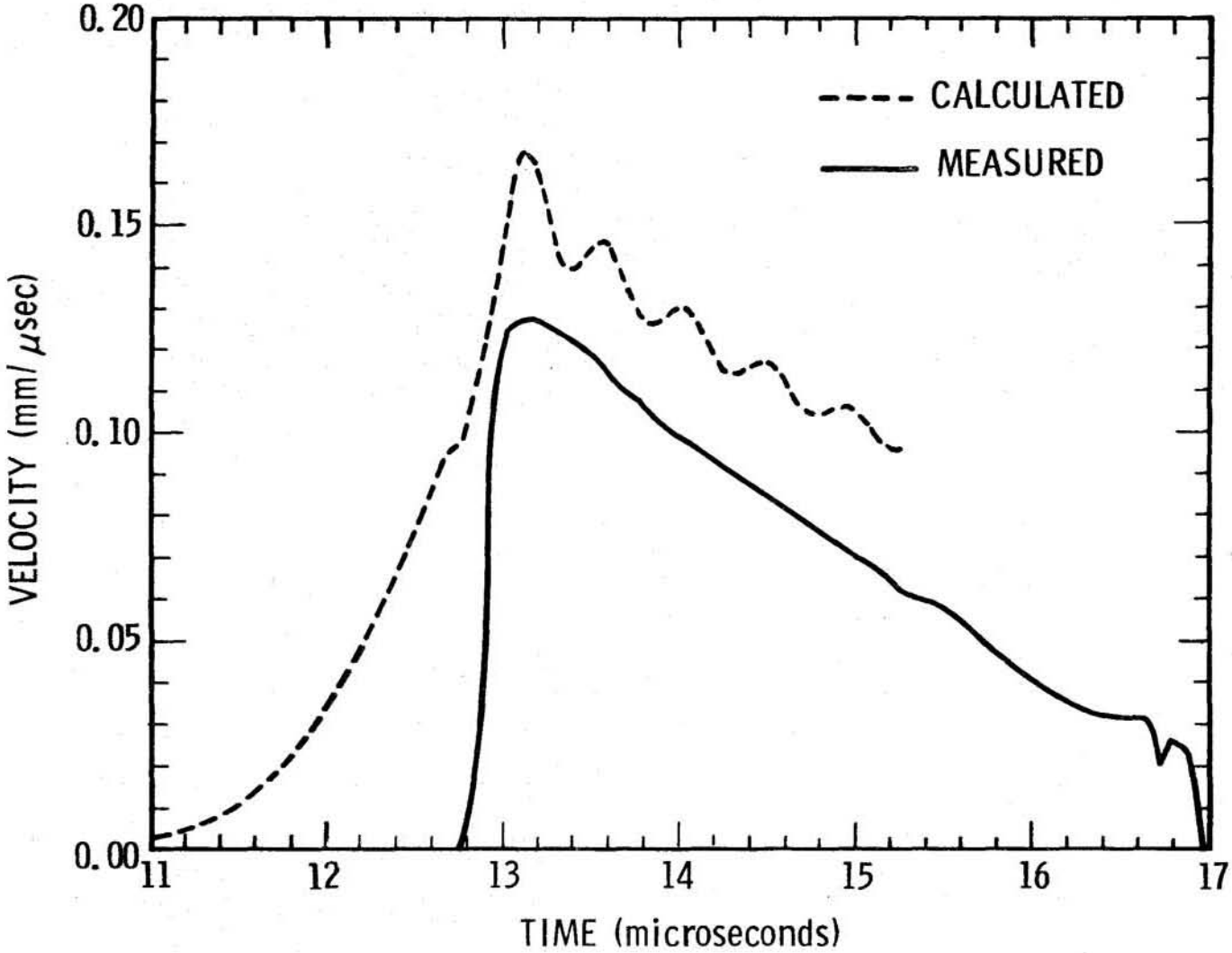


FIG. 19. COMPARISON OF VISCOELASTIC CALCULATION TO EXPERIMENTAL RECORD FOR THICK CONFIGURATION

UNLIMITED RELEASE

DISTRIBUTION:

J. O. Erkman
Naval Ordnance Lab
Silver Spring, MD 20910

D. J. Andrews
M.I.T.
Cambridge, MA 02139

T. J. Ahrens
CIT
Pasadena, CA 91109

Lynn Barker
Terra Tek, Inc.
Univ. Research Park
420 Wakara Way
Salt Lake City, UT 84108

P. C. Chou
Drexel Inst. Tech.
Philadelphia, PA 19104

Rodney Clifton
Brown University
Providence, RI 02916

Ian Fyfe
Univ. Washington
Seattle, Washington

Y. Horie
N. Carolina State U.
Raleigh, NC 27607

S. P. Marsh, M-6
Los Alamos Scientific Laboratory
Los Alamos, NM 87544

R. G. McQueen, M-6
Los Alamos Scientific Laboratory
Los Alamos, NM 87544

T. Michaels
General Motors Test Center
Warren, MI 48090

S. Sack, L-24
Lawrence Livermore Laboratory
P. O. Box 808
Livermore, CA 94550

J. D. Wackerle, WX-7
Los Alamos Scientific Laboratory
Los Alamos, NM 87544

G. E. Duvall
Dept. Physics
Washington State University
Pullman, WA 99163

M. L. Wilkins, L-24
Lawrence Livermore Laboratory
P. O. Box 808
Livermore, CA 94550

1280 T. B. Lane
1281 S. W. Key
1282 T. G. Priddy
1284 R. T. Othmer
2310 C. B. McCampbell
2314 J. J. Marron
2314 G. E. Clark
2314 R. K. Treece
2315 J. E. Gover
2315 S. T. Montgomery
2350 J. C. Crawford
2513 D. B. Hayes
2513 J. E. Kennedy
5000 A. Narath
Attn: 5200 E. H. Beckner
5400 A. W. Snyder
5700 J. H. Scott
5800 R. S. Claassen
5100 J. K. Galt
Attn: 5110 F. L. Vook
5120 G. J. Simmons
5150 J. E. Schirber
5130 G. A. Samara
5131 L. W. Davison
5131 P. J. Chen
5131 J. W. Nunziato
5160 W. Herrmann
5162 L. D. Bertholf
5162 W. T. Brown
5162 D. L. Hicks
5162 M. E. Kipp
5162 R. J. Lawrence
5162 J. W. Swegle (50)
5162 J. R. Tillerson
5162 W. E. Warren
5163 D. E. Munson

DISTRIBUTION: (Cont'd)
5163 D. E. Grady
5163 K. W. Schuler
5166 A. J. Chabai
5166 R. K. Byers
5166 W. R. Davey
5166 S. L. Thompson
5166 P. Yarrington
5167 B. M. Butcher
5734 A. L. Stevens
5734 R. R. Boade
8120 W. E. Alzheimer
8266 Tech. Library (2)
3141 Tech. Library (5)
3151 Tech. Writing (3)
For ERDA/TIC (Unlimited Release)
ERDA/TIC (25)
(R. P. Campbell 3171-1)